Turkish Journal of Chemistry

http://journals.tubitak.gov.tr/chem/

Research Article

Turk J Chem
(2015) 39: 1025 – 1037

doi:10.3906/kim-1410-37

Synthesis, characterization, and electrical and optical properties of magnesium-type boracite

Tuğba İBROŞKA[1], Azmi Seyhun KIPÇAK[1], Süreyya AYDIN YÜKSEL[2], Emek DERUN[1,*], Sabriye PİŞKİN[1]

[1]Department of Chemical Engineering, Faculty of Chemical and Metallurgical Engineering, Yıldız Technical University, İstanbul, Turkey

[2]Department of Physics, Faculty of Arts and Science, Yıldız Technical University, İstanbul, Turkey

Received: 17.10.2014 • **Accepted/Published Online:** 09.04.2015 • **Printed:** 30.10.2015

Abstract: Synthesis of the magnesium type of the mineral boracite ($Mg_3B_7O_{13}Cl$) was studied. Several parameters affecting boracite synthesis were investigated. The raw materials selected were magnesium chloride hexahydrate ($MgCl_2.6H_2O$), magnesium oxide (MgO), and boron oxide (B_2O_3). Reaction temperatures were selected between 600 °C and 900 °C. Moreover, three different reaction times of 4, 1, and 0.5 h were studied with the determined optimum molar ratio, reaction temperature, and reaction medium. Synthesized boracite characterization analyses were done by the techniques of X-ray diffraction (XRD), Fourier transform infrared spectroscopy (FT-IR), and scanning electron microscope (SEM). Reaction yields were also calculated. From the results of this study the magnesium type of boracite was obtained as a single phase with high XRD crystal score. Optimum conditions for the synthesis were as follows: $MgCl_2.6H_2O$ to B_2O_3 mole ratios of 5:6.5, 5:7.5, 6:6.5, 6:7.5, 7:6.5, 7:7.5; 600 °C reaction temperature; 1 h reaction time; and reaction medium as air atmosphere. Reaction yields were between 58.81 ± 1.65% and 77.49 ± 1.86%. Some selected magnesium type of boracite minerals, electrical resistivity, and optical absorbance properties were also measured for the determination of physical properties.

Key words: Magnesium-type boracite, solid-state synthesis, reaction yield

1. Introduction

Magnesium borates have many advantages in the boron mineral groups including their high elasticity coefficient and heat resistance, light weight, and anticorrosive properties.[1−4] With these properties magnesium borates can be used in cathode ray tube screens, in the ceramic industry, in detergent compositions, in ferroelastic material production, in fluorescent discharge lamps as luminescent materials, in friction reducing additive manufacture, as thermoluminescent phosphor, in superconducted material production, and in X-ray screens.[5−10]

There are several studies on the solid-state synthesis of magnesium-type borates in the literature. In these studies, the synthesis was conducted in a high temperature furnace. The magnesium sources mainly used were magnesium oxide (MgO), magnesium chloride hexahydrate ($MgCl_2{\cdot}6H_2O$), magnesium nitride hexahydrate $Mg(NO_3)_2{\cdot}6H_2O$, and magnesium hydroxide ($Mg(OH)_2$), and these sources were reacted with the boron sources of boron oxide (B_2O_3) and boric acid (H_3BO_3). In these syntheses dehydrated magnesium borate compounds were formed.[11−16]

*Correspondence: moroydor@yildiz.edu.tr

$Mg_2B_2O_5$ was obtained by Qasrawi et al. at 1250 °C with a 3 h reaction time using the reactants $Mg(OH)_2$ and H_3BO_3 [11], by Dosler et al.[12] at 1000 °C with the reactants MgO and B_2O_3, by Elssfah et al. at 900 °C using the same reactants used by Qasrawi et al.[13], by Li et al.[14] at 800 °C using the starting materials $MgCl_2{\cdot}6H_2O$ and $NaBH_4$, by Zeng et al. at 1200 °C in a vacuum for 1 h with a mixed tablet of $Mg(BO_2)_2$.[15] $Mg_3B_2O_6$ is another type of magnesium borate that can be synthesized via the solid-state method. This was studied by Zhang et al. with varying lengths and widths ranging between 100 and 300 nm[16] and Dosler et al. at 1300 °C with the same reactants of MgO and B_2O_3 that synthesize $Mg_2B_2O_5$ type of magnesium borate.[12]

Boracite is a borate compound that contains chlorine. Boracite is generally expressed by the formul $M_3B_7O_{13}X$. M represents the two valence cations of Mg, Cr, Mn, Fe, Co, Ni, Cu, Zn, or Cd and X is the one valence anion of F, Cl, Br, I, OH, or NO_3.[17] In some situations, X can be S, Se, or Te and M may be single valence Li.[18] In nature there are four types of boracite. These are ericaite and trembathite, with the same formulae of $(Fe,Mg)_3B_7O_{13}Cl$; chambersite ($Mn_3B_7O_{13}Cl$); and congolite ($Fe_3B_7O_{13}Cl$) $(Mg,Fe)_3B_7O_{13}Cl$).[19,20] Boracite is found with gypsum ($CaSO_4.2H_2O$), gypsum anhydrite ($CaSO_4$), halite (NaCl), sylvite (KCl), carnallite ($KMgCl_3.6(H_2O)$, kainite ($MgSO_4.KCl.3H_2O$), and hilgardite ($Ca_2B_5O_9Cl.H_2O$).[21]

Usually boracites were synthesized through four different methods, namely hydrothermal, pressurized mechanical, vapor transfer, and sintering flow.[20] The most widely used method was the sintering flow method. Using this method, Wang et al. synthesized the Fe–Cl type boracite.[22] On the other hand, Ju et al. studied the utilization of the flow method in boracite synthesis where they synthesized the five different halogen boracites $Mn_3B_7O_{13}Cl$, $Co_3B_7O_{13}Cl$, $Ni_3B_7O_{13}Cl$, $Cu_3B_7O_{13}Cl$, and $Zn_3B_7O_{13}I$ by the reaction of the transition metal halides $CoCl_2{\cdot}6H_2O$, $NiCl_2{\cdot}6H_2O$, $MnCl_2{\cdot}4H_2O$, $CuCl_2{\cdot}2H_2O$, and ZnI_2 together with H_3BO_3 at temperatures between 240 and 300 °C and reaction times between 2 and 4 days.[23]

In the study by Delfino et al., Ni–Br, Zn–Br, Zn–Cl, Mn–Cl, Co–Br, Mg–Cl, and Mn–I type boracites were studied at temperatures between 475 and 540 K, along with very long reaction times of 18–60 h and high reaction pressures of 5–33 atm.[24] However, in this study only the air atmosphere was studied and the reaction yield of magnesium-type boracite was not calculated.

In the literature, it is seen that the synthesis of magnesium type of boracites was not studied in detail, and that very long reaction times were employed, ranging from 2 to 4 days. Our study group conducted some preliminary research on boracite synthesis. For instance, some studies were carried out with the solid-state method, using H_3BO_3 as the raw material along with MgO and $MgCl_2{\cdot}6H_2O$, but the formation of pure boracite could not be achieved.[25,26] Another solid-state method employed at 1000 °C by Piskin et al. showed that at high temperatures, dehydrated type of magnesium borates were formed as the major phases.[25] In the study by Kipcak et al., the same raw materials were used as in the aforementioned study, but a lower temperature range of 500–700 °C was used. The results showed that the formation of boracite started at 500 °C; however, a further increase in temperature again resulted in the formation of dehydrated type of magnesium borates as the major phases.[26] Another important result obtained from these studies is that the use of H_3BO_3 in boracite synthesis was not suitable.

This study mainly focused on the solid-state rapid synthesis of magnesium type of boracites. For this aim several different parameters such as reaction temperature, reaction time, reaction atmosphere, and different types of raw materials were studied for optimization of the perfect crystal structure for magnesium type of boracites. After the synthesis, the characterization of the products was conducted using the techniques of

X-ray diffraction (XRD), Fourier transform infrared spectroscopy (FT-IR), and scanning electron microscope (SEM). Furthermore, with the selected magnesium type of boracite minerals, electrical resistivity and optical absorbance properties were measured.

2. Results and discussion

2.1. Raw material results

In the XRD analyses, the raw materials of $MgCl_2.6H_2O$ and MgO were identified as bischofite with JCPDS card number 01-077-1268 and periclase with JCPDS card number 01-087-0651. B_2O_3 is identified as the mixture of both phases of B_2O_3 and B_2O with JCPDS card numbers 00-006-0297 and 01-088-2485, respectively.

2.2. XRD results of the synthesized minerals

2.2.1. Stage 1

In stage 1, set 1 and set 2 syntheses were conducted using MgO (Mo), $MgCl_2.6H_2O$ (Mc), and B_2O_3 (B) with the synthesis temperature between 600 °C and 900 °C in air atmosphere. From the results of this stage three different phases were obtained (Table 1).

Table 1. XRD scores of the products synthesized from Mo, Mc, and B between 600 °C and 900 °C and 4 h of reaction time in air atmosphere (stage 1).

Sets	Mole ratio	600 °C			700 °C			800 °C			900 °C		
	(Mo:Mc:B)	B	M	S	B	M	S	B	M	S	B	M	S
1	4:1:6.5	16	45	-	21	50	20	65	67	20	21	77	26
	4:1:7.0	25	51	-	17	53	17	31	66	-	33	74	24
	4:1:7.5	7	50	-	20	53	19	23	55	22	32	78	25
	5:1:6.5	11	42	-	27	60	19	6	25	-	10	80	20
	5:1:7.0	30	53	-	26	52	20	17	65	-	34	78	23
	5:1:7.5	17	36	-	23	58	19	3	22	-	17	75	24
	6:1:6.5	19	43	-	23	60	-	23	62	-	20	79	21
	6:1:7.0	19	43	-	24	62	18	31	66	-	34	72	23
	6:1:7.5	6.5	52	-	20	52	17	4	21	17	26	78	22
2	4:2:6.5	25	21	-	23	47	18	10	39	25	38	72	23
	4:2:7.0	20	34	17	32	41	17	7	63	17	36	81	28
	4:2:7.5	24	12	-	20	50	16	22	65	21	34	77	23
	5:2:6.5	33	18	-	23	48	17	7	11	7.5	33	74	22
	5:2:7.0	34	31	-	29	52	22	3	61	25	34	76	21
	5:2:7.5	29	41	-	28	26	-	4	47	20	38	79	27
	6:2:6.5	24	26	-	19	39	17	17	53	28	42	77	27
	6:2:7.0	24	6.5	-	18	44	16	7	32	18	35	81	23
	6:2:7.5	24	32	-	33	50	22	7	47	20	39	75	25
3	0:5:6.5	60	23	-	63	50	-	65	67	21	42	70	21
	0:5:7.0	53	11	-	66	50	-	60	57	20	33	73	19
	0:5:7.5	55	29	-	63	69	-	59	69	-	31	68	22
	0:6:6.5	75	-	-	67	27	-	66	70	-	41	34	22
	0:6:7.0	62	51	-	65	54	-	66	67	-	26	65	24
	0:6:7.5	63	52	-	69	50	-	53	72	18	19	69	8
	0:7:6.5	64	3	-	69	52	-	67	72	-	44	76	-
	0:7:7.0	58	6	-	66	42	-	71	64	20	52	72	22
	0:7:7.5	68	-	-	67	51	-	62	63	19	40	71	20

These phases are 01-071-0750 JCPDS card numbered boracite ($Mg_3B_7O_{13}Cl$), 00-031-0787 JCPDS card numbered magnesium borate (MgB_4O_7), and 01-073-2107 JCPDS card numbered suanite ($Mg_2B_2O_5$). In the set 1 experiments, the magnesium borate (M) phase was seen as the major phase. The M phase's crystal scores increased with increasing reaction temperature. The highest M score of 80 was found in the 900 °C experiments with a 5:1:6.5 mole ratio (Mo:Mc:B). The B phase's crystal scores were lower than the M scores, which means that the B phase was the minor phase in the obtained products. Therefore, some of the Cl in the Mc reacted with hydrogen in air and turned to HCl; thus Mc is the limiting reactant and the excess amount of magnesium in both Mc and Mo turned to M phase. In set 2 experiments, the Mc amount was doubled. From the XRD results it is seen that doubling the Mc ratio increased B phase's score only a little. Again the M phase was seen as the major phase, with the highest crystal score of 81 at 900 °C again for both ratios of 4:2:7.0 and 6:2:7.0. In set 3 experiments, the Mo was removed from the raw materials, and the ratio of Mc was increased. In the products obtained from Mc and B, mainly the major phase was found as M at the reaction temperatures of 800 °C and 900 °C, while the major phase was found as B at the reaction temperatures of 600 °C and 700 °C. The desired pure boracite synthesis was accomplished at 600 °C in the ratios of 6:6.5 and 7:7.5.

2.2.2. Stage 2

In stage 2, the effect of reaction medium was investigated in the synthesis and the XRD results are shown in Table 2.

Table 2. Comparison of the XRD scores of the products synthesized from Mc and B at 600 °C and 900 °C and 4 h of reaction time in air and inert atmospheric conditions (stage 2).

Mole ratio	600 °C - Air			600 °C - Inert			900 °C - Air			900 °C - Inert		
(Mc:B)	B	M	S	B	M	S	B	M	S	B	M	S
5:6.5	60	23	-	54	6	-	65	67	21	22	23	-
5:7.0	53	11	-	56	10	-	60	57	20	10	65	-
5:7.5	55	29	-	52	16	-	59	69	-	16	68	-
6:6.5	75	-	-	58	-	-	66	70	-	21	38	19
6:7.0	62	51	-	59	21	-	66	67	-	35	73	-
6:7.5	63	52	-	55	7	-	53	72	18	34	76	-
7:6.5	64	3	-	55	-	-	67	72	-	59	62	-
7:7.0	58	6	-	56	10	-	71	64	20	34	36	-
7:7.5	68	-	-	58	-	-	62	63	19	29	74	27

Inert atmosphere was conducted using argon gas flow of 2 mL min^{-1}. Since the best results were obtained in stage 1 at 600 °C, the inert atmosphere experiments were conducted at 600 °C. The highest study temperature of 900 °C was also used. In the results of the inert atmosphere experiments, the B formation scores were decreased at the 600 °C reaction temperature. At the 900 °C reaction temperature both B and M phases' scores were also decreased. Thus, it is seen that the inert atmosphere conditions affect the synthesis conditions negatively.

2.2.3. Stage 3

After stage 1 and stage 2 experiments the best formation for the boracite synthesis was seen at 600 °C and partly in 700 °C, and so in stage 3 three new reaction temperatures (650 °C, 550 °C, 500 °C) were used. XRD results of the stage are given in Table 3.

Table 3. XRD scores of the products synthesized from Mc and B between 500 °C and 650 °C and 4 h of reaction time in air atmosphere (stage 3).

Mole ratio	500 °C		550 °C		600 °C		650 °C	
(Mc:B)	B	M	B	M	B	M	B	M
5:6.5	33	-	66	3	60	23	63	6
5:7.0	34	1	59	3	53	11	60	7
5:7.5	34	-	57	3	55	29	51	6.5
6:6.5	44	1	66	3	75	-	57	8
6:7.0	45	1	60	3	62	51	63	10
6:7.5	34	-	64	3	63	52	59	-
7:6.5	43	1	68	3	64	3	56	8
7:7.0	44	-	65	-	58	6	69	3
7:7.5	31	-	65	3	68	-	65	12

At the temperature of 650 °C, like at 600 °C, the formation of M was the minor phase. The pure B phase was seen at the mole ratio of 6:7.5 only with an XRD score of 59. Mainly at 650 °C the B scores were decreased a little. At 550 °C reaction temperature M phase scores decreased to 3 and the pure B phase was seen only at the mole ratio of 7:7.0. At 500 °C, M phase scores decreased to 1 and B phase scores also decreased. The decrease in the B phase indicated that the B phase formation begins at the 500 °C reaction temperature. Among all of the syntheses again the 600 °C reaction temperature yielded the best results for boracite synthesis.

2.2.4. Stage 4

In stage 4 the effect of the reaction time on boracite synthesis was investigated by keeping the reaction temperature and atmospheric condition constant as 600 °C and air, respectively. Among the results obtained, which are given in Table 4, in 1 h reaction time pure boracite was synthesized at the mole ratios of 5:6.5, 5:7.5, 6:6.5, 6:7.5, 7:6.5, and 7:7.5.

Table 4. XRD scores of the products synthesized from Mc and B at 600 °C and 0.5–4 h of reaction time in air atmosphere (stage 4).

Mole ratio	0.5 h		1.0 h		4.0 h	
(Mc:B)	B	M	B	M	B	M
5:6.5	63	-	65	-	60	23
5:7.0	60	7	66	5	53	11
5:7.5	61	16	63	-	55	29
6:6.5	68	-	69	-	75	-
6:7.0	69	4	64	3	62	51
6:7.5	62	5	67	-	63	52
7:6.5	66	4	70	-	64	3
7:7.0	67	4	64	5	58	6
7:7.5	68	-	67	-	68	-

The highest XRD score of 70 was obtained with the mole ratio of 7:6.5. In addition, at the reaction time of 0.5 h pure boracite formation occurred at some of the mole ratios but the XRD scores were smaller than at the 1 h reaction time. Pure boracite phases' XRD patterns obtained at 600 °C reaction temperature and 1 h reaction time and the crystallographic data of both boracite and magnesium borate are given in Figure 1 and Table 5, respectively.

Table 5. Crystallographic data of the synthesized minerals.

Mineral name	Boracite	Magnesium borate	Suanite
JCPDS card no.	01-071-0750	00-031-0787	01-073-2107
Chemical formula	$Mg_3B_7O_{13}Cl$	MgB_4O_7	$Mg_2B_2O_5$
Molecular weight (g/mole)	392.03	179.55	150.23
Crystal system	Orthorhombic	Orthorhombic	Monoclinic
Space group	Pca21 (no. 29)	Pbca (no. 61)	P21/a (no. 14)
a (Å)	8.5496	8.5960	12.1000
b (Å)	8.5496	13.7290	3.1200
c (Å)	12.0910	7.9560	9.3600
α (°)	90.00	90.00	90.00
β (°)	90.00	90.00	104.33
γ (°)	90.00	90.00	90.00
z	4.00	8.00	4.00
Density (calculated) ($g.cm^{-3}$)	2.95	2.54	2.91

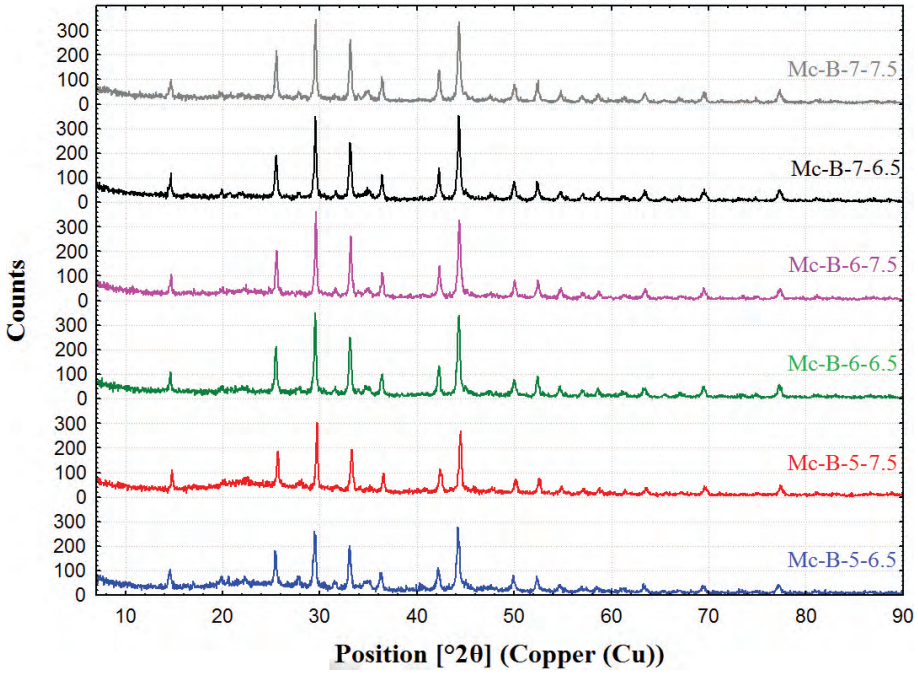

Figure 1. XRD patterns of the synthesized magnesium type of boracite minerals with Mc:B ratios of 5:6.5, 5:7.5, 6:6.5, 6:7.5, 7:6.5, and 7:7.5.

In Figure 1, it is seen that the major peaks of boracite are found at 14.6, 25.5, 29.5, 33.1, 36.4, 42.4 and 44.3°, which correspond to Miller indices of (002), (202), (004), (222), (132), (224), and (233), respectively.

2.3. FT-IR results

The FT-IR spectra of the synthesized minerals at 600 °C reaction temperature and 1 h reaction time are given in Figure 2.

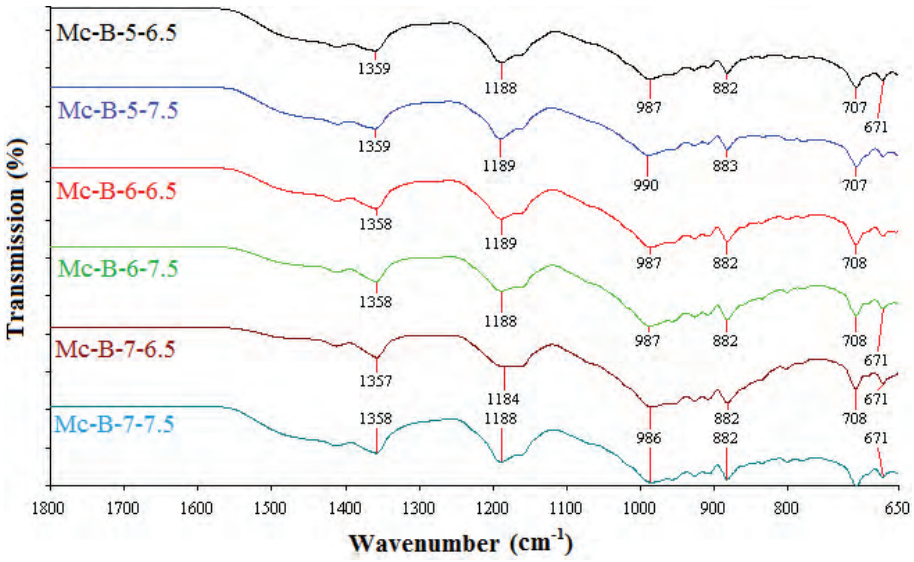

Figure 2. FT-IR spectra of the synthesized magnesium type of boracite minerals with Mc:B ratios of 5:6.5, 5:7.5, 6:6.5, 6:7.5, 7:6.5, and 7:7.5.

Since there were no peaks were observed above 1800 cm^{-1}, spectral range was given in the range of 1800–650 cm^{-1}. The peaks at the wavenumber of 1359–1357 cm^{-1} and 1189–1184 cm^{-1} correspond to the asymmetrical stretching of the 3-coordinate boron [ν_{as}($B_{(3)}$-O)]. The asymmetrical stretching of the 4-coordinate boron [ν_{as}($B_{(4)}$-O)] and symmetrical stretching of the 3-coordinate boron [ν_{s}($B_{(3)}$-O)] are seen at the peaks between 990 and 986 cm^{-1} and 883 and 882 cm^{-1}, respectively. The last peaks between 708 and 671 cm^{-1} correspond to the bending of the 3-coordinate boron [δ($B_{(3)}$-O]. From the peaks obtained it is seen that the characteristic boron to oxygen bands were formed in the synthesis and these bands are in mutual agreement with Yongzhong et al.[27]

2.4. SEM morphologies

SEM morphologies of the pure boracites synthesized at 600 °C reaction temperature and 1 h reaction time are given in Figure 3.

At the ratio of 5:6.5 (Figure 3a), flower type transparent layers crystals are seen and the particle sizes are in the range of 397.31–768.98 nm. At the ratio of 5:7.5 (Figure 3b) the crystals consist of majorly solid and round crystals and a few transparent flower type crystals, the particle sizes of which are 322.59–754.91 nm. Some tubular crystals along with solid round type crystals are seen at the ratio of 6:6.5 (Figure 3c), where the particle sizes are 390.16–662.91 nm. At the ratio of 6:7.5 (Figure 3d), like 5:7.5 solid and round crystals are seen but at this ratio the products are agglomerated and form large crystals. The particle sizes are between 305.23 and 842.29 nm at the ratio of 6:7.5. At 7:6.5 (Figure 3e) round solid crystals are agglomerated and form large crystals like at 6:7.5, where their particle sizes are between 386.54 and 705.81 nm. At the last ratio of 7:7.5 (Figure 3f), some flower like crystals and solid round and rectangular crystals are formed, with particle sizes between 450.78 and 735.33 nm. The smallest and largest particle sizes are seen at the ratios of 6:7.5 and 6:7.5, respectively.

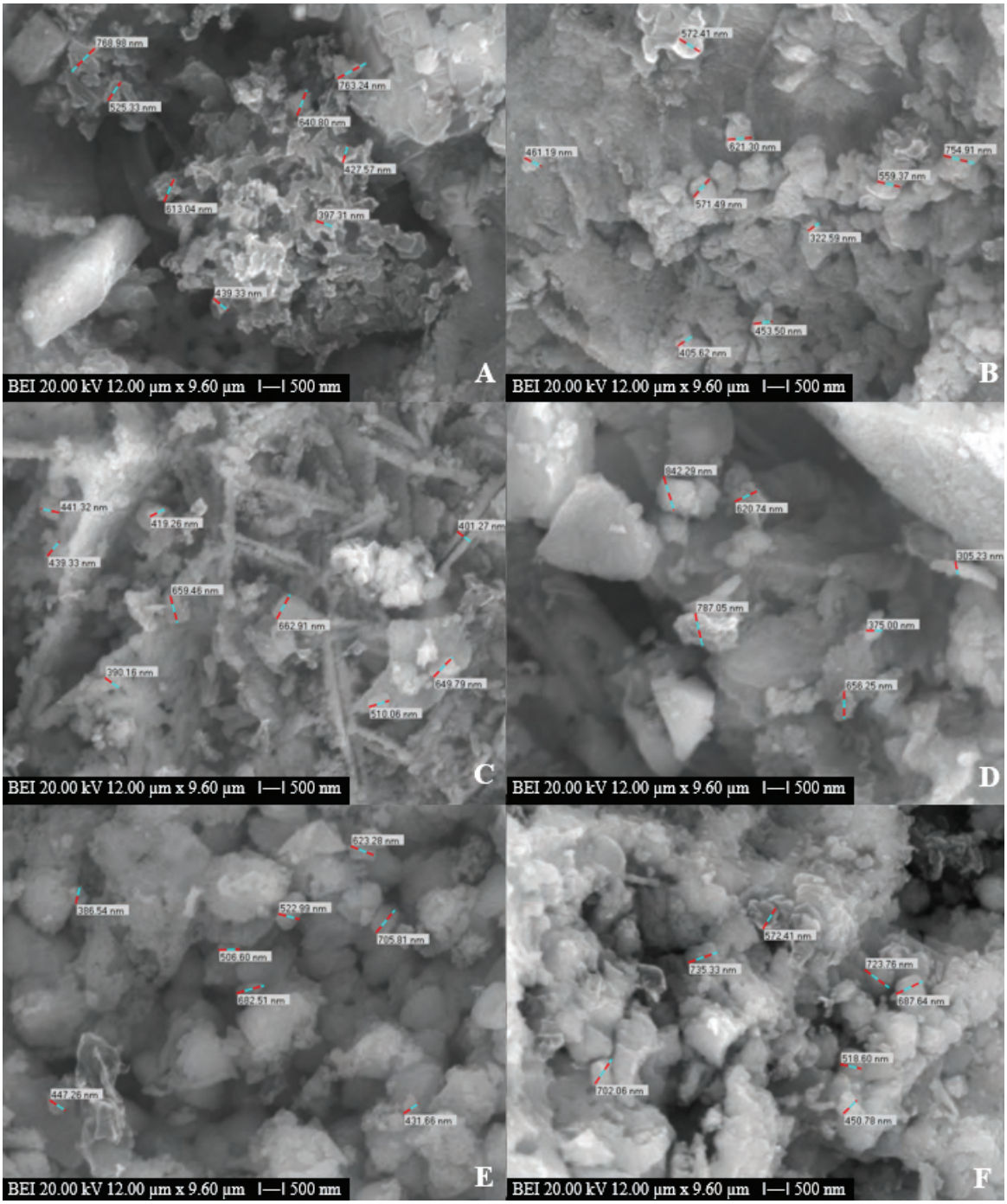

Figure 3. SEM morphologies of the synthesized magnesium type of boracite minerals with Mc:B ratios of a. 5:6.5, b. 5:7.5, c. 6:6.5, d. 6:7.5, e. 7:6.5, f. 7:7.5.

2.5. Reaction yields

The reaction yields calculated for the pure boracites synthesized at 600 °C reaction temperature and 1 h reaction time are shown in Figure 4. The highest and lowest reaction yields are seen at the mole ratios of 6:7.5 and 5:6.5 with values of 77.49 ± 1.86% and 58.81 ± 1.65%, respectively.

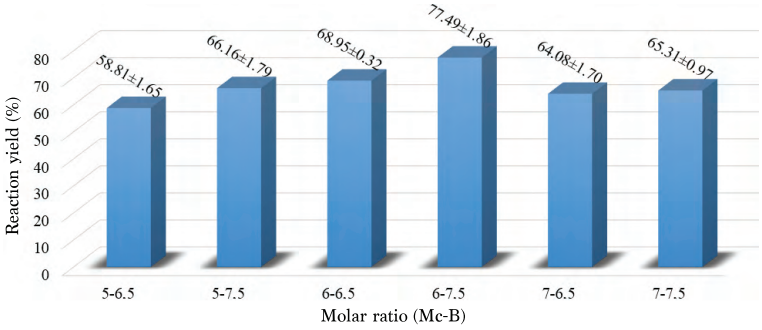

Figure 4. Reaction efficiencies of the synthesized magnesium type of boracite minerals with Mc:B ratios of 5:6.5, 5:7.5, 6:6.5, 6:7.5, 7:6.5, and 7:7.5.

2.6. Electrical and optical measurement results

Figure 5 shows the current voltage characteristics of the magnesium type of boracite mineral with Mc:B mole ratios of 5:7.5, 6:7.5, and 7:7.5; 600 °C reaction temperature; and 1 h reaction time. The resistivity of magnesium type of boracite minerals at Mc:B mole ratios of 5:7.5, 6:7.5, and 7:7.5 are 9.10×10^6, 1.75×10^6, and $1.50 \times 10^5 \Omega.\mathrm{cm}$, respectively, obtained from the current voltage curves. By increasing the ratio of Mc in boracite formation, electrical resistivity decreased from 9.10×10^6 to 1.50×10^5 $\Omega.\mathrm{cm}$. The resistivity of boracite minerals has not been studied in the literature but the conductivity of magnesium borate nanowires was calculated as 10^{-4} $(\Omega.\mathrm{m})^{-1}$ by Lee et al.[28] Since the conductivity is inversely proportional to resistivity, the resistivity of the magnesium borates was about 10^7 $\Omega.\mathrm{cm}$. Therefore, the electrical conductivities of the pure boracites were lower than those of the magnesium borates.

The absorption spectra of the magnesium type of boracite mineral with Mc:B mole ratios of 6:7.5 and 7:7.5 were measured in the wavelength range of 200–1000 nm at room temperature. Figure 6 shows the optical absorption spectra of the magnesium type of boracite minerals.

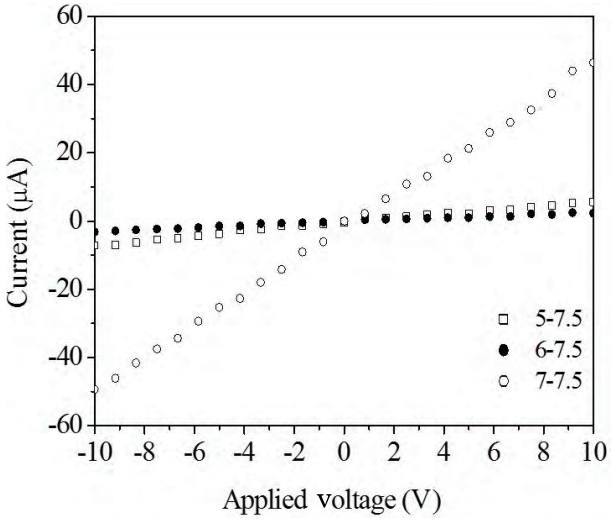

Figure 5. The current voltage characteristics of magnesium type of boracite minerals with Mc:B ratios of 5:7.5, 6:7.5, and 7:7.5.

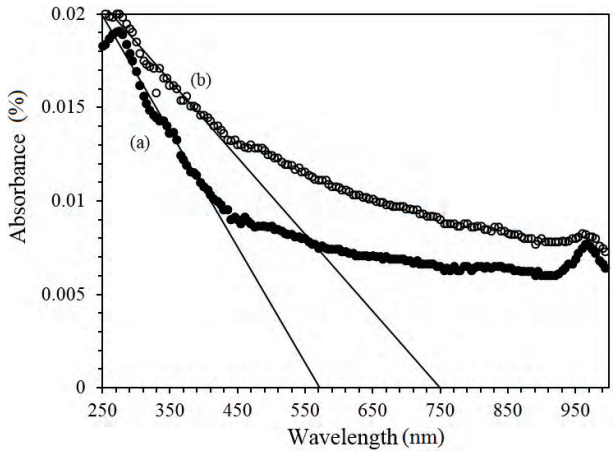

Figure 6. The optical absorption spectra of the magnesium type of boracite mineral with Mc:B ratios of a, 6:7.5, b, 7:7.5.

The optical energy gap of the magnesium type of boracite mineral was determined from extrapolation of the high energy part of absorption spectra as about 2.18 eV–1.65 eV, respectively. The optical energy gap of the magnesium type of boracite mineral decreased with increasing Mc ratio from 6:7.5 to 7:7.5. As with electrical resistivity, boracite minerals' optical energy gap has not been studied but the energy band gap of magnesium borates was calculated to be 4.72 eV by Kumari et al.[29]

In conclusion, in this study the magnesium type of boracite synthesis via solid-state method was examined. The study was started with the raw materials $MgCl_2.6H_2O$, MgO, and B_2O_3 and the pure boracite was obtained from the $MgCl_2.6H_2O$ and B_2O_3. The optimization of several parameters was revealed as the pure high crystal scored boracites were synthesized at the conditions of 600 °C reaction temperature, 1 h reaction time, in air atmosphere, and at molar ratios of 5:6.5, 5:7.5, 6:6.5, 6:7.5, 7:6.5, and 7:7.5. For comparison with the literature studies, reaction times of the magnesium type boracite synthesis were decreased, leading to high energy conservation. Also from the results, electrical resistivity values and optical energy gaps of magnesium-type boracites were 9.10×10^6–$1.50 \times 10^5 \Omega.cm$ and 2.18 eV–1.65 eV.

3. Experimental

3.1. Materials

$MgCl_2.6H_2O$ (CAS Number 7791-18-6) and MgO (CAS Number 1309-48-4) were purchased from Sigma-Aldrich with a minimum purity of 99%, and B_2O_3 was purchased from Eti Mine Bandirma Boron Works with a minimum purity of 98%. When $MgCl_2.6H_2O$ was used for both magnesium and chlorine sources, MgO was used for the magnesium source and B_2O_3 was used for the boron source in the experiments. Since the obtained MgO and B_2O_3 particle sizes were below 325 mesh (44 μm) and 18 mesh (1 mm), B_2O_3 was ground in an agate mortar (Retsch RM 200) and sieved through 200 mesh (74 μm) to reduce the particle size. $MgCl_2.6H_2O$ is highly capable of taking moisture from air and so it was not pretreated. After the pretreatment the raw materials were identified in a Philips PANalytical X-Pert Pro XRD with a Cu Kα tube working with the conditions of 45 kV and 40 mA and range of the patterns was set between 7 and 90°.

3.2. Synthesis methods

At the beginning of the study some preexperiments were conducted for the determination of molar ratios.[30] Then some other molar ratios were added. Along with the synthesis method, several parameters were studied; in stage 1 experiments, the reaction temperatures were between 600 and 900 °C (the temperature increment was 10 °C/min), reaction time was 4 h, and the mole ratios of the raw materials were between 4 and 6 for MgO (Mo), 1 for $MgCl_2.6H_2O$ (Mc), and between 6.5 and 7.5 for B_2O_3 (B) in set 1, considering the theoretical synthesis if any of the side products were not produced as given in Eq. (1):

$$MgCl_2.6H_2O(s) + 5MgO(s) + 7B_2O_3(s) + Air(g) \overset{heat}{\rightarrow} 2\,(Mg_3B_7O_{13}Cl)\ (s) + 6H_2O(g) \tag{1}$$

However, considering that HCl gas will be produced in the system, the chlorine to be used in synthesis will be stoichiometrically less in proportion; thus the formation of dehydrated magnesium borate minerals would be expected in addition to the synthesis of boracite (Eq. (2)).

$$\begin{aligned} &MgCl_2.6H_2O(s) + 5MgO(s) + 7B_2O_3(s) + Air(g) \overset{heat}{\rightarrow} \\ &a\,(Mg_3B_7O_{13}Cl)\ (s) + bH_2O + cHCl(g) + dMg_xB_yO_z(s) \end{aligned} \tag{2}$$

The ratio of Mc was increased in set 2. After the set 2 synthesis dehydrated magnesium borate minerals were also seen. Thus in set 3 experiments Mo was removed from the raw materials and the ratio of Mc is increased to 5–7 (Mo ratio added to Mc). The expected formation is given in Eq. (3):

$$6\,(MgCl_2.6H_2O)\;(s) + 7B_2O_3(s) + Air(g) \overset{heat}{\rightarrow} 2\,(Mg_3B_7O_{13}Cl)\;(s) + 31H_2O + 10HCl(g) \qquad (3)$$

In the stage 2 experiments, the atmospheric conditions were studied to determine how the boracite synthesis is affected. The top (900 °C) and bottom temperatures (600 °C) of stage 1 (bottom temperature gave the best formation in stage 1) were selected. In the experiments argon gas flow (2 mL min^{-1}) was used for obtaining inert atmosphere. After experimenting with different atmospheric conditions that affect the synthesis, the reaction temperatures in stage 3 were decreased below to 500 °C, in order to determine the boracite formation temperature. In the last stage, stage 4, different reaction times were studied.

Before the synthesis for the preparation of the pellets, homogeneous mixtures were subjected to Manfredi OL 57 pellet preparation equipment with 100 bar pressure. Then the pellets were reacted in a Protherm MOS 180/4 high temperature furnace in alumina dust covered ceramic crucibles. After the synthesis, products were ground in a ceramic mortar. The scheme of the experiments is given in Figure 7.

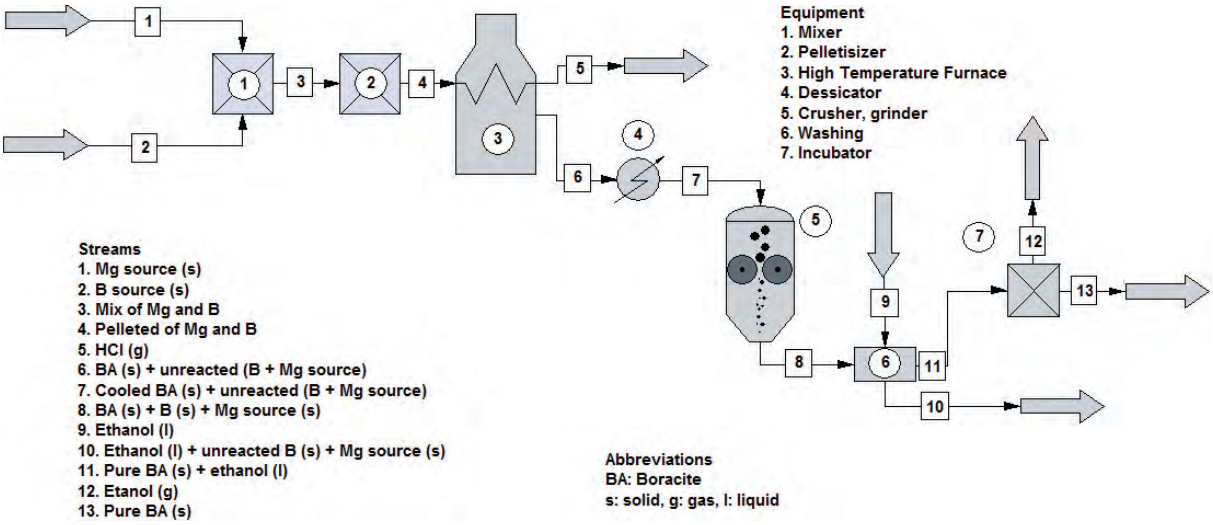

Figure 7. Schematic representation of the reaction system.

3.3. Characterization of the boracite

The characterizations of the formed products were carried out using XRD, FT-IR, and SEM techniques. XRD analyses were conducted with the parameters given in section 3.1. Furthermore, the XRD scores (when all of the peak intensities (%) and peak locations matched perfectly with the JCPDS card number of reference mineral, the XRD score of analyzed mineral is equal to 100) were analyzed.

A PerkinElmer Spectrum One FT-IR with a universal attenuated total reflectance (ATR) sampling accessory, diamond/Zn, was used for the determination of the characteristic bands of products. Scan number and resolution parameters were selected as 4 and 4 cm^{-1}, respectively, in the FT-IR analyses.

The synthesized products' surface morphologies and particle sizes were determined by a CamScan Apollo 300 Field-Emission SEM working at 20 kV. The scale of magnification was in the range of 10,000 and back-scattering electron (BEI) detector was used.

Yield analysis was also performed using methods reported previously.[31–35] For the pure boracites, $MgCl_2.6H_2O$ and B_2O_3 were identified as the key components depending on the limiting reactants. Experimental runs were performed in triplicate.

The number of moles of product at the final stage, N_D, was divided by the number of consumed moles of the key reactant A to calculate the overall yield, Y_D (Eq. (4)). The number of moles of A consumed was calculated using the initial (N_{A0}) and final (N_A) moles of the reactant. For a batch system, the equation then becomes[36]

$$Y_D = \frac{N_D}{N_{A0} - N_A} \tag{4}$$

3.4. Electrical and optical properties

Some synthesized magnesium-type boracite minerals were pressed into pellets under pressure of 30 MPa with 13 mm diameters and about 0.4–0.5 mm thickness. Electrical resistivity measurement of selected magnesium-type boracite minerals, which were synthesized with the mole ratios of 5:7.5, 6:7.5, and 7:7.5; $MgCl_2.6H_2O$ to B_2O_3 mole ratios; 600 °C reaction temperature; and 1 h reaction time, were carried out by standard current voltage measurement at room temperature using a Keithley 6487 in darkness with thermally evaporated silver contacts on both surfaces of pellets. The absorption spectra of the magnesium-type boracite minerals were recorded using a PerkinElmer ultraviolet-visible spectrophotometer in the wavelength range of 250–1000 nm at room temperature. In this measurement the magnesium-type boracite minerals were dispersed in HCl solution with the same concentration in a quartz tube (1 cm × 1 cm).

References

1. Dou, L.; Zhong, J.; Wang, H. *Phys. Scripta* **2010**, *T139*, 014010.
2. Li, S.; Xu, D.; Shen, H.; Zhou, J.; Fan, Y. *Mater. Res. Bull.* **2012**, *47*, 3650–3653.
3. Kumari, L.; Li, W. Z.; Kulkarni, S.; Wu, K. H.; Chen, W.; Wang, C.; Vannoy, C. H.; Leblanc, R. M. *Nanoscale Res. Lett.* **2010**, *5*, 149–157.
4. Xu, B.; Li, T.; Zhang, Y.; Zhang, Z.; Liu, X.; Zhao J. *Cryst. Growth. Des.* **2008**, *8*, 1218–1222.
5. Shahare, D. I.; Dhoble, S. J.; Moharil, S. V. *J. Mater. Sci. Lett.* **1993**, *12*, 1873–1874.
6. Hu, Z. S.; Lai, R.; Lou, F.; Wang, L. G.; Chen, Z. L.; Chen, G. X.; Dong J. X. *Wear* **2002**, *252*, 370–374.
7. Kashiwada, Y.; Furuhata, Y. *Phys. Status Solidi A* **1976**, *36*, K29–K31.
8. Wang, H.; Jia, G.; Wang, Y.; You, Z.; Li, J.; Zhu, Z.; Yang F.; Wei, Y.; Tu, C. *Opt. Mater.* **2007**, *29*, 1635–1639.
9. Furetta, C.; Kitis, G.; Weng, P. S.; Chu, T. C. *Nucl. Instrum. Methods Phys. Res. A* **1999**, *420*, 441–444.
10. Zhu, W.; Zhang, Q.; Xiang, L.; Wei, F.; Sun, X.; Piao, X. *Cryst. Growth Des.* **2008**, *8*, 2938–2945.
11. Qasrawi, A. F.; Kayed, T. S.; Mergen, A.; Gürü, M. *Mater. Res. Bull.* **2005**, *40*, 583–589.
12. Došler, U.; Kržmanc, M. M.; Suvorov, D. *J. Eur. Ceram. Soc.* **2010**, *30*, 413–418.
13. Ellsfah, E. M.; Enousi, A.; Zhang, J.; Song, H. S.; Chengcun, T. *Mater. Lett.* **2007**, *61*, 4358–4361.
14. Li, S.; Fang, X.; Leng, J.; Shen, H.; Fan, Y.; Xu, D. *Mater. Lett.* **2010**, *64*, 151–153.
15. Zeng, Y.; Yang, H.; Fu, W.; Qiao, L.; Chang, L.; Chen, J.; Zhu H.; Li, M; Zou, G. *Mater. Res. Bull.* **2008**, *43*, 2239–2247.
16. Zhang, J.; Li, Z.; Zhang, B. *Mater. Chem. Phy.* **2006**, *98*, 195–197.
17. Mao, S. Y.; Schmid, H.; Triscone, G.; Muller, J. *J. Magn. Magn. Mater.* **1999**, *199*, 65–75.

18. Li, D.; Xu Z. J.; Wang, Z. H.; Geng, D. Y.; Zhang, J. S.; Zhang, Z. D.; Yuan, G. L.; Liu, J. M. *J. Alloys Compd.* **2003**, *351*, 235–240.
19. Frost, R. L.; Xi, Y.; Scholz R. *Spectrochim. Acta, Part A*, **2012**, *96*, 946–951.
20. Castellanos-Guzman, A. G.; Trujillo-Torrez, M.; Czank, M. *Mater. Sci. Eng.* **2005**, *120*, 59–63.
21. Frost, R. L.; Lopez, A.; Scholz, R., Xi, Y. *Spectrochim. Acta, Part A* **2014**, *120*, 270–273.
22. Wang, Z. H.; Geng, D. Y.; Li, D.; Zhao, X. G.; Zhang, Z. D. *J. Alloys Compd.* **2001**, *329*, 278–284.
23. Ju, J.; Li, H.; Wang, Y.; Lin, J.; Dong, C. *J. Mater. Chem.* **2002**, *12*, 1771–1774.
24. Delfino, M.; Gentile, P. S.; Gabriel, M. L.; Smith, W. A. *Method for the Synthesis of Boracides*; US Patent no: 4.243.642, 1981.
25. Piskin, S.; Gurel, S. E.; Senberber, F. T.; Kipcak, A. S.; Derun, E. M.; Tugrul, N. *Journal of International Scientific Publications: Materials, Methods and Technologies* **2013**, 7, 362–372.
26. Kipcak, A. S.; Ibroska, T.; Tugrul, N.; Derun, E. M.; Piskin, S. *Sigma, Journal Of Engineering And Natural Sciences* **2014**, *32*, 201–210.
27. Yongzhong, J.; Shiyang, G.; Shuping, X.; Jun, L. *Spectrochim. Acta, Part A* **2000**, *56*, 1291–1297.
28. Li, Y.; Fan, Z.; Lu, J. G.; Chang, R. P. H. *Chem. Mater.* **2004**, *16*, 2512–2514.
29. Kumari, L.; Li, W. Z.; Kulkarni S.; Wu, K. H.; Chen, W.; Wang, C.; Vannoy, C. H.; Leblanc, R. M. *Nanoscale Res. Lett.* **2009**, *5*, 149–157.
30. Ibroska, T.; Kipcak, A. S.; Derun, E. M.; Piskin, S. In *Solid-State synthesis and characterization of boracite minerals at 800 ° C from $MgCl_2.6H_2O$, MgO and B_2O_3*. Proceedings of the First International Symposium on Innovative Technologies for Engineering and Science, Sakarya, Turkey, 2013.
31. Derun, E. M.; Kipcak A. S.; Senberber F. T.; Yilmaz, M. S. *Res. Chem. Intermediat.* **2015**, *41*, 853–866.
32. Kipcak, A. S.; Moroydor Derun, E.; Piskin, S. *J. Chem.* **2013**, 329238.
33. Kipcak, A. S.; Yilmaz Baysoy, D.; Moroydor Derun, E.; Piskin, S. *Adv. Mater. Sci. Eng.* **2013**, 747383.
34. Kıpçak, A. S.; Moroydor Derun, E.; Pişkin, S. *Turk. J. Chem.* **2014**, *38*, 792–805.
35. Kipcak, A. S.; Yildirim, M.; Yuksel, S. A.; Moroydor Derun, E.; Piskin S. *Adv. Mater. Sci. Eng.* **2014**, 819745.
36. Fogler, H. S. *Elements of Chemical Reaction Engineering*; 3rd edition, Prentice-Hall: Englewood Cliffs, NJ, USA, 1999.